Inversion of water cloud lidar signals based on accumulated depolarization ratio

Gilles Roy[1] and Xiaoying Cao[2]

[1]RDDC Valcartier, 2459 Pie XI North, Québec, Québec G3J 1X5, Canada;

[2]Department of Chemistry and Chemical Engineering, Royal Military College of Canada,Kingston, Ontario K7K 7B4, Canada; Xiaoying.Cao@rmc.ca

*Corresponding author: gilles.roy@drdc-rddc.gc.ca

Received 27 October 2009; revised 5 February 2010; accepted 5 February 2010; posted 18 February 2010 (Doc. ID 119102); published 15 March 2010

The relation between the accumulated single scattering factor and the layer accumulated depolarization ratio appears to be independent of the geometry of the measurements and contains information on the optical depth and thus on the extinction coefficient. A simple equation is developed to retrieve the extinction coefficient from the total integrated signal and the integrated depolarization ratio measurements. The results compare well with Klett and Weinman lidar inversion techniques. The results from the measurements of the integrated depolarization ratio can be used to set the far end initial extinction coefficient value required for Klett and Weinman lidar inversion or can be used directly. © 2010 Optical Society of America

OCIS codes: 010.3640, 290.4210.

1. Introduction

Hu *et al.* [1–3] have proposed a relationship between integrated single scattering fraction and accumulated linear depolarization ratio for water droplets. Cao *et al.* [4] extended the idea of the accumulated depolarization for circular polarization and proposed a unique relation between the integrated single scattering fraction and the depolarization parameter [5], which does not depend on whether linear or circular lidar polarization is being used. The relation between the accumulated single scattering factor (A_s) and the layer accumulated depolarization ratio appears to be independent of the geometry of the measurements and contains information on the optical depth and thus on the extinction coefficient. This suggests that a lidar inversion technique based on the Hu relationship and a generalized relationship could be derived to evaluate the extinction coefficient.

In this paper we show that Hu type relationships can be used to perform the inversion of the lidar signal from water clouds. It will be referred to as LAD (layer accumulated depolarization) inversion technique.

We first develop a lidar inversion equation based on the measurement of the integrated depolarization ratio. Then, using water cloud data with known optical depths obtained in a controlled environment, we compare the inversion results with those obtained from Klett [6] and Weinman [7] lidar inversion techniques. Finally the technique is applied to a real water cloud, and the sensitivity of the technique is discussed.

2. Derivation of the LAD Lidar Inversion Technique

The lidar equation is written as

$$P(z) = \frac{C}{z^2}\beta(z)\exp\left[-2\int_0^z \sigma(z')\mathrm{d}z'\right], \qquad (1)$$

where $C = P_0\frac{c\tau}{2}F(z)A$ is the lidar constant, where P_0 is the initial laser power released, τ is the laser pulse width, $F(z)$ is the overlapped area between laser source and receiver, and A is the collecting area.

0003-6935/10/091630-06$15.00/0

The backscattering coefficient, β, and the extinction coefficient, σ, are related via the backscattering-extinction ratio k, i.e., $\beta(z) = k\sigma(z)$.

In the following we consider a single-component atmosphere base on the assumption of the dominance of the scattering from the cloud droplets over other atmospheric constituents. Following Platt [8], the integrated range corrected single scattering signal is

$$I_s(z) = \int_0^z P(z')z'^2 \mathrm{d}z' = \int_0^z Ck\sigma(z') \exp\left(-2\int_0^{z'} \sigma(z'')\mathrm{d}z''\right)\mathrm{d}z'. \quad (2)$$

Since $\sigma(z')\mathrm{d}z' = -\mathrm{d}T'(z')/T'(z')$, we easily find that

$$I_s(z) = \frac{Ck}{2}(1 - T^2). \quad (3)$$

Independent as they are of the polarization (linear or circular), Hu relationships between the single scattering fraction A_s and the accumulated depolarization ratios are written for a given field of view (FOV), θ:

$$A_s(\theta) \equiv \frac{I_s(z)}{I_T(z,\theta)} = \frac{(1 - \delta_{\mathrm{acc_{lin}}}(z,\theta))^2}{(1 + \delta_{\mathrm{acc_{lin}}}(z,\theta))^2} = \frac{1}{(1 + \delta_{\mathrm{acc_{cir}}}(z,\theta))^2}, \quad (4)$$

where $\delta_{\mathrm{acc_{lin}}}$ and $\delta_{\mathrm{acc_{cir}}}$ are the accumulated linear and circular depolarization ratios, respectively, and $I_T(z)$ is the integrated lidar signal including multiple scattering (see [4,5] for a discussion of the harmonization of linear and circular polarization Hu relationships). We have

$$\delta_{\mathrm{acc}}(z,\theta) = \frac{\int_{z_a}^z P_{\perp T}(z',\theta)z'^2\mathrm{d}z'}{\int_{z_a}^z P_{//T}(z',\theta)z'^2\mathrm{d}z'}, \quad (5)$$

$$I_T(z,\theta) = \int_{z_a}^z (P_{//T}(z',\theta) + P_{\perp T}(z',\theta))z'^2\mathrm{d}z'. \quad (6)$$

$P_{//}$ and $P_\perp$ are the lidar returns parallel and perpendicular to the transmitted laser polarization.

Substituting Eq. (3) into Eq. (4), we have

$$T^2(z) = Ck - 2A_s(\theta)I_T(z,\theta). \quad (7)$$

Now considering two distances z_1 and z_2, with $z_2 = z_1 + \Delta z$, then

$$T^2(z_1) = \exp\left(-2\int_0^{z_1} \sigma(z')\mathrm{d}z'\right), \quad (8)$$

$$T^2(z_2) = \exp\left(-2\int_0^{z_2} \sigma(z')\mathrm{d}z'\right) = \exp\left(-2\int_0^{z_1} \sigma(z')\mathrm{d}z' - 2\int_{z_1}^{z_1+\Delta z} \sigma(z')\mathrm{d}z'\right). \quad (9)$$

Taking the natural logarithm on both sides of Eqs. (8) and (9) and setting $\bar{z} = (z_1 + z_2)/2$ we have

$$\ln(T^2(z_1)) - \ln(T^2(z_2)) = 2\sigma(\bar{z})(z_2 - z_1). \quad (10)$$

Using Eq. (7) in Eq. (10) we have the LAD lidar inversion:

$$\sigma(\bar{z}) = \frac{1}{2(z_2 - z_1)} \ln\left[\frac{Ck - 2A_s(\theta,z_1)I_T(z_1,\theta)}{Ck - 2A_s(\theta,z_2)I_T(z_2,\theta)}\right]. \quad (11)$$

Ck can be derived from Eq. (7) as

$$Ck = \frac{2A_s(z,\theta)I_T(z,\theta)}{1 - T^2(z)}. \quad (12)$$

The problem is that the transmission $T(z)$ is generally unknown. For dense water clouds, Hu *et al.* [2] set $T(z) = 0$ and determined C by setting $k = 1/18$. In the next section we will validate Eq. (11) using data obtained under a controlled environment.

3. Experimental Validation of Hu Lidar Inversion for Water Droplets

In this section, we present experimental results on water droplets to examine the validity of the LAD lidar inversion technique of Eq. (11). The experimental conditions are those described in [9]. In short, the measurements have been performed using a dual polarization multiple-field-of-view (MFOV) lidar. The MFOV lidar measurements were made in a 22 m long aerosol chamber located 105 m from the lidar. A transmissometer was used to measure the cloud's optical depth. The MFOV lidar operated at 532 nm. It consisted of a telescope coupled to a gated intensified CCD camera (G-ICCD) synchronized with a frequency doubled Nd-YAG laser polarized alternatively either linearly or circularly. For each preset distance, the camera recorded two images simultaneously, one for each polarization. The calculated encircled energy for a given FOV provides the lidar signal for a given distance. The delays applied to the G-ICCD camera were set to study the evolution of the lidar return as a function of the penetration depth into the aerosol chamber for five different ranges (106.7, 110.3, 114.0, 117.7, and 121.3 m, respectively, from the laser source). The data treatment is the same as in [4] to correct the laser beam spreading in the larger FOVs and the effects of imperfect optics.

First we need to calculate the value of Ck. This is done using Eq. (12), the transmissometer data, and the measured $A_s(z,\theta)I_T(z,\theta)$ at a distance

$z = 121.3$ m. (Since the transmittance T was located very close to the last measured layer at 121.34 m, the lidar system constant Ck is calculated on measurements at that layer.) Then using Eq. (11) the extinction is calculated for the five layers. For comparison purposes we have also calculated the extinction using the Klett [6] and Weinman [7] inversion techniques,

$$\sigma(z)_{\text{Klett}} = \frac{[S(z)/S(z_g)]}{\sigma^{-1}(z_g) + \frac{2}{k}\int_z^{z_g}(S(z')/S(z_g))\mathrm{d}z'}, \quad (13)$$

$$\sigma(z)_{\text{Weiman}} = \frac{[S(z)][1-\exp(-2\tau)]}{2\left\{\int_z^{z_g}[S(z')]\mathrm{d}z' + \exp(-2\tau)\int_{z_0}^{z}[S(z')]\mathrm{d}z'\right\}}. \quad (14)$$

The single scattering range corrected signal $S(z)$ was set equal to $\mathrm{d}I_s(z)/\mathrm{d}z$, with $I_s(z) = A(z,\theta)I_T(z,\theta)$ as in Eq. [4]. Klett and Weinman inversion techniques require an initial value to be estimated at the back end of the cloud. For Klett inversion the back end initial value was set equal to the value obtained with the LAD inversion technique. For Weinman's technique, the initial value is set with the optical depth as measured with the transmissometer. If the bounds of cloud can be determined, then Klett and Weinman inversion methods are theoretically the same.

Figure 1 shows the results of the LAD and Klett inversions when compared to the Weinman inversion results for independent measurements (seven linear polarizations and six circular polarizations). The agreement with the Weinman extinction is very good in both cases. The LAD inversion shows extinction values 6% smaller than the Weinman. As expected, the difference between the Klett and Weinman inversion is less than 0.4%.

4. Application on a Real Water Cloud and Discussion

Figures 2 and 3 show lidar returns for principal and secondary polarizations for a cloud layer starting at

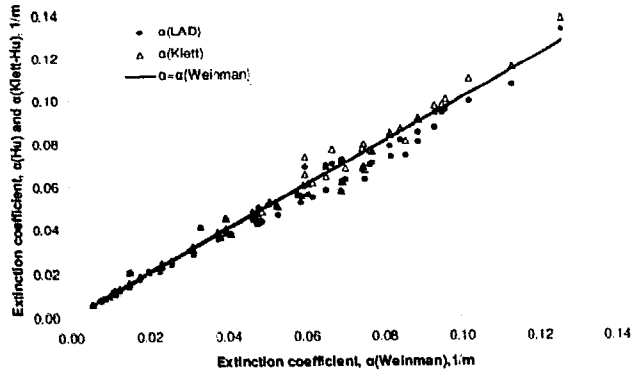

Fig. 1. (Color online) Calculated extinction coefficients from LAD and Klett lidar as a function of the extinction coefficient calculated using Weinman lidar inversion. The start extinction value for Klett inversion used the LAD estimation at the cloud end.

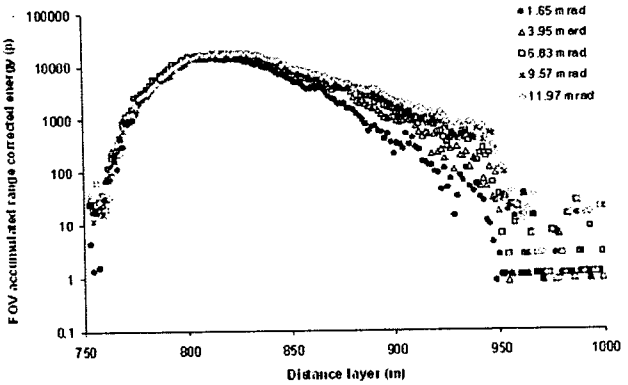

Fig. 2. (Color online) Range corrected parallel polarization lidar signal as a function of distance for five FOVs.

750 m and ending at 950 m. The fact that all the signals drop abruptly at the same distance (950 m) is an indication of the cloud ending at that very distance. The measurements were done at 1064 nm at a repetition rate of 100 Hz, and the different FOV measurements were performed sequentially in less than a second with a variable aperture. At small FOVs the secondary polarization signals do not go as deep into the cloud as the large FOVs, and solutions for the small FOVs will be restricted to distances where the signal does exist.

We easily verify that the integrated single scattering fraction as a function of the integrated depolarization ratio follows a Hu relationship. It is then possible to obtain the single scattering lidar signal I_s from the multiple scattering lidar signals using Eq. (4), $I_s(z) = A_s(\theta,z)I_T(\theta,z)$. Figure 4 shows the range corrected single scattering signals, $\mathrm{d}I_s(z)/\mathrm{d}z$, for FOVs ranging from 2.6 mrad to 12 mrad. All the derived single scattering signals superpose well. Under ideal conditions, the single scattering signal should superpose perfectly. The small differences are attributed to cloud changes; the measurements were not done simultaneously. Now that we are confident in the data set, we need to calculate the Ck value. To do so, we assume that, in the middle of the cloud, the cloud extinction coefficient is constant and we have

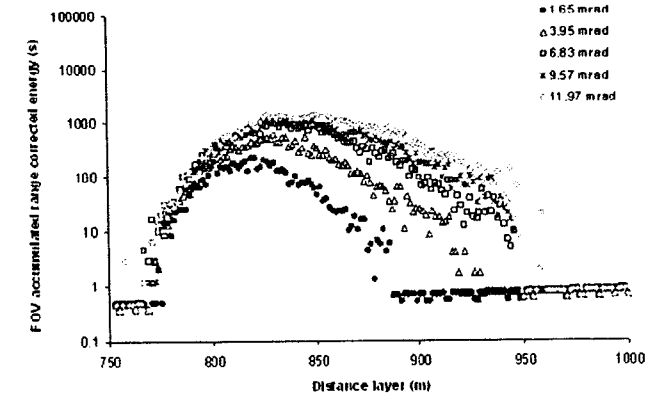

Fig. 3. (Color online) Range corrected perpendicular polarization lidar signal as a function of distance for five FOVs.

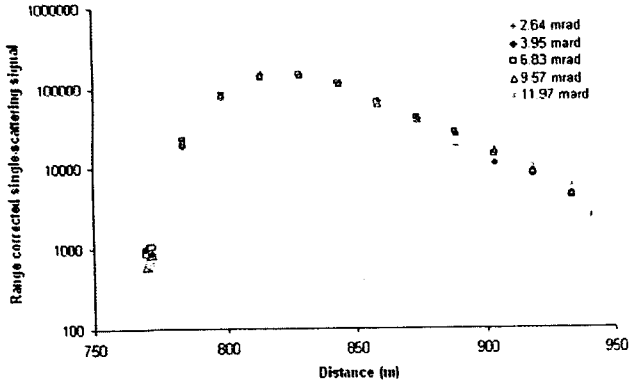

Fig. 4. (Color online) Range corrected single scattering signals, $I_s(z)$, superimpose well for five different FOVs. The difference is attributed to cloud fluctuation between the different measurements.

$$T^2(z_1,z_2)=\frac{(\mathrm{d}I_s(z=z_2)/\mathrm{d}z)}{(\mathrm{d}I_s(z=z_1)/\mathrm{d}z)}.$$

After rearrangement of Eq. (11) we have

$$Ck=\frac{2A_s(z_2,\theta)I_T(z_2,\theta)-2T^2(z_1,z_2)A_s(z_1,\theta)I_T(z_1,\theta)}{1-T^2(z_1,z_2)}. \tag{15}$$

The difference between Eqs. (12) and (15) is that in Eq. (12) the transmission is the transmission through the whole cloud up to position z, while in Eq. (15) the transmission is calculated between two specific positions z_1 and z_2.

The determination of Ck is critical for the proposed inversion method. Under ideal conditions, Ck should have a single value. Because C is proportional to the laser power, it will show the same fluctuation. Ck values have been calculated using Eq. (15) for distances $z_1=833$ m and $z_2=888$ m for each of the measurements performed at the different FOVs, and then LAD lidar inversion has been performed using Eq. (11) for the cloud ranging from 760 m to 940 m; the results are shown in Fig. 5. The retrieved extinction values agree well up to two thirds of the cloud; the last third of the cloud shows higher dispersion in the values. A simple look at the LAD lidar inversion [Eq. (11)] reveals that exact values of the constant Ck do not have the same importance at the beginning and at the end of the cloud. A larger variance at large optical depths is due to the fact $2A_s(z,\theta)I_T(z,\theta)$ tends to reach a value practically equal to Ck; in fact, $2A_s(z,\theta)I_T(z,\theta)=Ck$ for $T(z)=0$, rendering Eq. (11) ill conditioned for these cases. The consequence is that a small error on the estimation of Ck or a small fluctuation in the product $2A_s(z,\theta)I_T(z,\theta)$ is sufficient to create large fluctuations in the retrieved value. At the beginning of the cloud, because $2A_s(z,\theta)I_T(z,\theta)\ll Ck$, a small error in the Ck value has little effect. Finally the large discrepancy observed for the FOVs larger than 10 mrad is most likely caused by improper radial calibration of the detectors; at these large FOVs the light is focused on the edge of the detector. The reason why the discrepancy due to this miscalibration effect is not seen at smaller values of the depth into the cloud is that, at these earlier depths, the multiple scattering events that send photons into the larger FOVs are much less numerous.

Figure 6 compares the averaged retrieved extinction values as a function of distance for the LAD, Klett, and Weinman inversion techniques, respectively. To do so, the LAD extinction results are averaged over all the FOVs as well as the optical depth up to a distance of 930 m (the outlier data point for a FOV of 12 mrad at a distance of 910 m has been ignored). The extinction coefficient obtained from the LAD technique at the back end of the cloud (930 m) is used as initial value for Klett lidar inversion, and the calculated optical depth at the same distance is used for the Weinman lidar inversion. The agreement between the different inversion techniques is good.

To show the sensitivity of the LAD lidar inversion over the Ck values, the calculations were redone with Ck values ranging from $0.98\,Ck$ to $1.02\,Ck$. The results are displayed in Fig. 7. We observe a clear departure of the different solutions at the end of

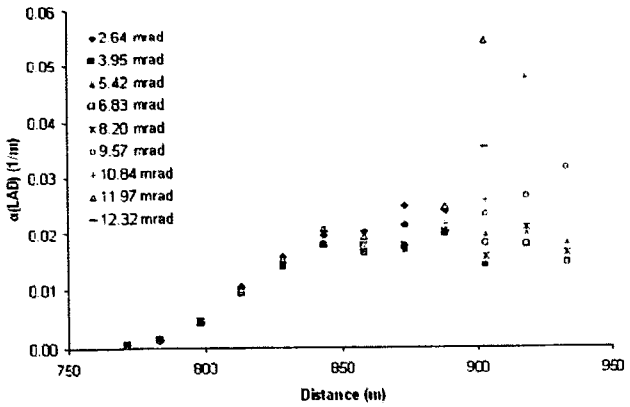

Fig. 5. (Color online) Calculated extinction coefficients obtained using the LAD lidar inversion as a function of distance for all the FOVs considered. For larger penetration depths, solutions do not exist for all FOVs.

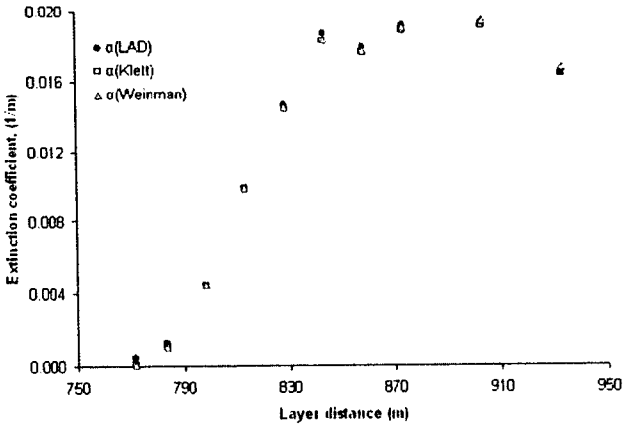

Fig. 6. (Color online) Comparison of the retrieved extinction coefficients for LAD, Klett, and Weinman lidar inversion methods.

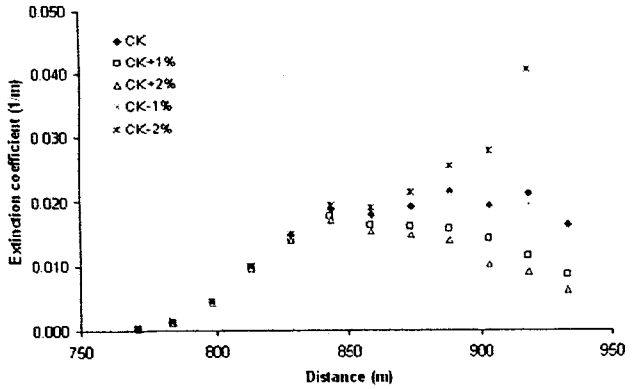

Fig. 7. (Color online) Comparison of the retrieved extinction coefficients for LAD inversion technique for five different values of Ck.

the cloud. The fact that the extinctions still agree well at the beginning of the cloud is an indication that the front end of the cloud is not very sensitive over Ck values as previously discussed. The Klett and Weiman inversion results are not shown in this graph, but they follow rigorously the LAD inversion data for all cases.

For Ck values smaller by 2%, inversion results do not exist for large penetration depths (solutions for $2A_s(z,\theta)I_T(z,\theta) \geq Ck$ do not exist).

Using Eq. (15) for different distances z_1 and z_2 we found that a precision of 1% is achievable on Ck values. Considering that for optical depths smaller than 2.3, a Ck value smaller by 1% than the true value leads to no solution, we are confident that the LAD inversion technique will provide good results for optical depths less than 2. Methods to improve the value of Ck need to be investigated for larger optical depths. Possibly an iterative method as suggested by Platt [10] could be used. In that context, the larger FOVs should be considered because they show the higher secondary polarization signal. Also, the limit of Ck can be estimated from the retrieval process: wrong Ck will lead to an apparently wrong solution. But this is not always straightforward to identify a "wrong solution," especially for Ck larger than the right value, as shown in Fig. 7.

Usually ground based atmospheric lidar uses FOVs close to or smaller than 1 mrad. A FOV of 1 mrad is too small to collect a significant amount of multiple scattering leading to an important depolarization signal. Measurements performed with FOVs larger than 3 mrad are required. Also, larger FOVs will provide higher cloud penetration depths.

Since the LAD inversion compares well to the Klett and Weinman inversions, we can simply use LAD inversion to provide an optical depth value to the Weinman or Klett inversion technique. But also, LAD inversion technique is self-consistent, and lidar inversion can be obtained directly at any distance inside the cloud from it; it is not necessary to start from the end of the cloud.

Because of the particular geometry of a space lidar, its signal contains a strong proportion of multiple scattered light even for FOVs smaller than 0.1 mrad, and consequently application of the LAD inversion technique is most likely directly applicable.

In order to work properly, the LAD inversion technique requires good relative calibration of two detectors. This can be easily performed by the introduction of a half-wave plate before the polarization cube that splits the two polarizations. Doing so, it inverts the polarization incident on the detectors, and the relative calibration is obtained. Also, because the measurements are performed on large FOVs, the radial responses of the detectors must be calibrated relative to the responses at their centers. This is accomplished by measuring the lidar signal obtained by illuminating a solid target with a small laser beam at different off-axis FOVs. Doing so, it assures sufficient accuracy on the measurements.

5. Conclusion

Hu *et al.* [1–3] have established an empirical relation between the accumulated single scattering factor and the layer accumulated depolarization ratio that is independent of the geometry of the measurements and contains information on the optical depth and thus on the extinction coefficient. Although empirical, the Hu relationship was proven to be highly accurate. This has suggested the derivation of a lidar inversion technique based on the Hu relationship and the assignment of the initial values required by Klett and Weinman lidar inversions based on the measurement of the integrated depolarization ratio.

In this paper we have done the following:

- Developed a simple lidar inversion technique (LAD) to retrieve the extinction coefficient from the total integrated signal and the integrated depolarization ratio.
- Validated the LAD inversion technique with Klett and Weinmann lidar inversion techniques using a lidar signal obtained under controlled environment.
- Applied the LAD inversion technique to real cloud data and used LAD inversion data as input parameters for Klett and Weinmann lidar inversion.
- Determined that the LAD inversion technique provides good results for optical depths less than 2; for higher optical depths, further refinement on the inversion technique is required.

The material presented in this paper is valid for water droplets clouds. Generalization of the present work to nonspherical particles is not easy and will require the elaboration of a Hu type relationship for other types of particles [4]. Possibly Monte Carlo simulations on cirrus clouds could open new research avenues.

The authors wish to thank Robert Bernier from "Les instruments optiques du St-Laurent (IOSL) for helpful discussions and comments.

References

1. Y. Hu, Z. Liu, D. Winker, M. Vaughan, V. Noel, L. Bissonnette, G. Roy, and M. McGill, "Simple relation between lidar multiple scattering and depolarization for water clouds," Opt. Lett. **31**, 1809–1811 (2006).
2. Y. Hu, M. A. Vaughan, D. M. Winker, Z. Liu, V. Noel, L. Bissonnette, G. Roy, M. McGill, and C. R. Trepte, "A simple multiple scattering-depolarization relation of water clouds and its potential applications," presented at the 23rd International Laser Radar Conference, Nara, Japan, 24–28 July 2006, pp. 19–22.
3. Y. Hu, M. Vaughan, Z. Liu, B. Lin, P. Yang, D. Flittner, B. Hunt, R. Kuehn, J. Huang, D. Wu, S. Rodier, K. Powell, C. Trepte, and D. Winker, "The depolarization-attenuated backscatter relation: CALIPSO lidar measurements vs. theory," Opt. Express **15**, 5327–5332 (2007).
4. X. Cao, G. Roy, N. Roy, and R. Bernier, "Comparison of the relationships between lidar integrated backscattered light and accumulated depolarization ratios for linear and circular polarization for water droplets, fog-oil and dust," Appl. Opt. **48**, 4130–4141 (2009).
5. G. G. Gimmestad, "Reexamination of depolarization in lidar measurements," Appl. Opt. **47**, 3795–3802 (2008).
6. J. D. Klett, "Stable analytical inversion solution for processing lidar returns," Appl. Opt. **20**, 211–220 (1981).
7. J. A. Weinman, "Derivation of atmospheric extinction profiles and wind speed over the ocean from a satellite-borne lidar," Appl. Opt. **27**, 3994–4001 (1988).
8. C. M. R. Platt, "Lidar and radiometric observations of cirrus clouds," J. Atmos. Sci. **30**, 1191–1204 (1973).
9. G. Roy and N. Roy, "Relation between circular and linear depolarization ratios under multiple scattering conditions," Appl. Opt. **47**, 6563–6579 (2008).
10. C. M. R. Platt, "Remote sounding of high clouds. I: Calculation of visible and infrared optical properties from lidar and radiometer measurements," J. Appl. Meteor. **18**, 1130–1143 (1979).